# Composite Pulses

**Malcolm H. Levitt**
*Stockholm University, Sweden*



Turn, turn, turn. (The Byrds)

## 1 INTRODUCTION

A composite pulse is a small number of contiguous, or near-contiguous, rf pulses with different phase. The composite pulse emulates the effect of a simple rf pulse, but has an inbuilt compensatory mechanism which renders it less sensitive to common experimental imperfections. Composite pulses may be compensated against the inevitable spread in the amplitude of the applied rf field over a sample of finite extent; they may be rendered insensitive to the limited strength of the applied rf field compared with the interactions of the spins with each other (spin–spin couplings) or with the molecular electron clouds (chemical shifts). In some cases other common pulse imperfections such as pulse shape errors are compensated. Composite pulse sequences are useful in a wide range of experimental situations in NMR. They are particularly important when critical experiments are performed in difficult situations, such as when the sample is large compared with the rf coil, absorbs rf fields strongly, or when the attainable field is restricted because heating must be avoided.

A case of particular importance is broadband heteronuclear spin decoupling (see ***Decoupling Methods***). Here a continuous train of composite pulses is applied to one spin species while a different spin species is observed. Suitable composite pulse sequences cause the spin system to evolve as if the heteronuclear spin–spin couplings were absent. The minimization of heating effects is particularly demanding in this application since the rf field may be applied continuously over a period of seconds. Composite pulse techniques have allowed a large reduction in the usable rf power and are now almost universal in heteronuclear liquid state NMR.

Compensation of the nuclear spin dynamics is also important in solid state NMR. Controlled spin manipulations can be achieved even when the achievable rf field is comparable with

For list of General Abbreviations see end-papers

magnetic dipole–dipole couplings or electric quadrupole couplings. They are used in quadrupole echo experiments, methods to determine the orientation dependence of spin–lattice relaxation times, and for heteronuclear decoupling. Composite pulses have also been designed for NMR in zero magnetic field[1] (see ***Zero Field NMR***), in nuclear quadrupole resonance (NQR) spectroscopy[2,3] and even in coherent optical experiments.[4–6]

The original idea of compensating rf pulses for imperfections has been extended in several additional directions.

1. Composite pulses have been designed with an *exaggerated* sensitivity to the rf field amplitude. The response with respect to the rf field strength may be tailored so that there is strong uniform excitation within a given range and minimal excitation otherwise. In combination with careful rf coil design, such composite pulses comprise a means of spatial localization (see ***Localization by Rotating Frame Techniques***) of the nuclear spin signal.
2. Composite pulses have been designed with a carefully-tailored *frequency response*, i.e. dependence of spin dynamics on chemical shifts. This can be used, for example, in the suppression of undesirable NMR signals from solvent spins (see ***Water Suppression in Proton MRS of Humans & Animals***).
3. Composite pulses may be constructed which simulate the effect of arbitrary rf phase shifts on spectrometers which are equipped only to produce 90° phase steps.
4. Many experiments in coupled spin systems require some knowledge of the typical values of spin–spin coupling constants or quadrupole couplings. In practice, there is some spread in the magnitudes of these interactions, leading to a reduced experimental efficiency or, in some cases, extra peaks in two-dimensional spectra. By making analogies with composite pulses, methods have been designed which are internally compensated against deviations of the couplings from their expected values.
5. Composite pulse sequences closely related to heteronuclear decoupling sequences are widely used for the propagation of spin coherence through extended networks of spin–spin couplings.

The variety of composite pulse sequences, and the range of associated theoretical approaches and applications, is large. The choice of topics covered here is necessarily subjective. A more detailed, and theoretical, review of the field up to 1986 is given by Levitt.[7]

## 2 NOTATION

Consider a spin species $I$ with magnetogyric ratio $\gamma_I$, exposed to a strong static magnetic field $\boldsymbol{B}_0$. The Larmor frequency of the spins, neglecting for the moment chemical shifts and spin–spin couplings, is given by $\omega_0 = -\gamma_I B_0$, in units of rad $s^{-1}$. For example, the Larmor frequency $\omega_0/2\pi$ for protons in a field $B_0 = 11.74$ T is approximately −500 MHz.

During an rf pulse, an additional oscillating magnetic field is applied. The oscillation frequency of the applied field will be denoted by $\omega_1$ (this conforms to the notational convention used in this Encyclopedia, but the reader is warned against conflicts with much published work). Usually $\omega_1$ is very close to the Larmor frequency of the spins $\omega_0$.

For high-field NMR, the relevant component of the rf magnetic field is perpendicular to the static magnetic field, and rotates around $\boldsymbol{B}_0$ in the same sense as the precessional motion of the spins. The *amplitude* of the relevant component of the oscillating rf field is denoted by $B_1$. This is usually written in terms of the *nutation frequency*

$$\Omega_1 = -\gamma_I B_1 \tag{1}$$

The nutation frequency $\Omega_1/2\pi$ is usually of the order of kilohertz or tens of kilohertz, and is generally assumed to be positive for convenience (for spins with positive $\gamma_I$, this implies that the field component $B_1$ is taken to be negative).

In general, $\Omega_1$ is spatially inhomogeneous, i.e. differs from place to place in the sample. This will sometimes be stressed by writing $\Omega_1(\boldsymbol{r})$, where $\boldsymbol{r}$ is a spatial coordinate.

To set the pulse durations it is necessary to assume a certain 'nominal' nutation frequency $\Omega_1^0$. This represents roughly the most probable value of $\Omega_1$ over the sample volume, and is normally determined by some simple experimental procedure. For example, the '90° pulse length' $\tau_{90}$ can be set by finding the pulse duration giving the maximum NMR signal. The nominal nutation frequency $\Omega_1^0$ is then defined through the relationship:

$$\Omega_1^0 \tau_{90} = \pi/2 \tag{2}$$

Other experimental procedures may give slightly different estimates. This does not matter very much. $\Omega_1^0$ should simply be somewhere near the center of the actual $\Omega_1(\boldsymbol{r})$ distribution.

The *duration* $\tau_p$ of a single rf pulse is conveniently denoted in terms of $\Omega_1^0$ by the 'nominal flip angle' $\beta_p^0$, defined by

$$\beta_p^0 = \Omega_1^0 \tau_p \tag{3}$$

A rectangular rf pulse can therefore be specified by using the two angles $\beta_p^0$ (for the duration) and $\phi_p$ (for the rf phase), and will be denoted $(\beta_p^0)_{\phi p}$, with the angles given in degrees. Otherwise, radians will be used. For example, $90_{45}$ denotes a rectangular rf pulse with an rf phase $\phi_p = \pi/4$ and a pulse duration $\tau_p = (\pi/2)/\Omega_1^0$.

A composite pulse is simply a sequence of single rectangular pulses. For simplicity, only *contiguous* composite pulses will be considered here, i.e. there are no spaces between the pulses. All component pulses are assumed to have the same frequency, although this is not always the case in practice.[8] The composite pulse sequence is written in chronological order from left to right. For example, $90_{45}180_0$ denotes a rectangular rf pulse with rf phase of $\pi/4$ and a duration of $\tau_p = (\pi/2)/\Omega_1^0$, immediately followed by another rectangular pulse with an rf phase of zero and a duration of $\tau_p = \pi/\Omega_1^0$.

Sometimes it is necessary to denote an overall phase shift of an entire group of pulses. This is done using square brackets, for example $[(\beta_1^0)_{\phi 1}\ (\beta_2^0)_{\phi 2}]_\Phi$, which is equivalent to $(\beta_1^0)_{\phi 1+\Phi}\ (\beta_2^0)_{\phi 2+\Phi}$.

A pulse sequence $\mathbb{S}$ with an element $\mathbb{E}$ missing at the front will be denoted by $\mathbb{E}^{-1}\mathbb{S}$. For example, if a sequence $\mathbb{S}$ is given by $\mathbb{S} = 90_{45}180_0 90_{180}$, then $(90_{45})^{-1}\mathbb{S}$ is given by $180_0 90_{180}$. Similarly, $\mathbb{S}(90_{180})^{-1}$ is given by $90_{45}180_0$. The pulse sequence $\mathbb{E}\ ^1\mathbb{S}\mathbb{E}$ derived from $\mathbb{S}$ by taking the element $\mathbb{F}$ from the front to the back is a *cyclic permutation* of $\mathbb{S}$.

The chronological reverse of a pulse sequence $\mathbb{S}$ is denoted by $\mathbb{S}^{\text{rev}}$. In the example above, $\mathbb{S}^{\text{rev}}$ would be $90_{180}180_0 90_{45}$.

For References see p. 1410

## 3 PULSE IMPERFECTIONS

Two common causes of imperfect pulse performance are: (i) lack of uniformity in the applied rf field, and (ii) limited amplitude of the rf field compared with the other interactions experienced by the spins.

### 3.1 Radiofrequency Field Inhomogeneity

The amplitude of the relevant rf field component varies from place to place in the sample. The rf field experienced by the spins is conveniently represented by the dimensionless parameter $\Omega_1/\Omega_1^0$, which is equal to 1.0 for the nominal rf field. In practice, $\Omega_1/\Omega_1^0$ deviates from unity by a few percent in a well-designed high-resolution NMR probe, but the deviations may exceed 20% for a surface coil in NMR imaging (see ***Surface Coil NMR: Quantification with Inhomogeneous Radiofrequency Field Antennas***).

### 3.2 Limited rf Field Amplitude

The usable rf field amplitude is always limited, either because sample heating must be minimized, or because of the risk of electrical failure in the amplifiers or rf coil. Magnetic fields associated with chemical shifts or spin couplings compete with the rf field during the pulse and bring about a degradation in pulse performance.

#### *3.2.1 Isotropic Liquids*

In isotropic liquids, spin–spin couplings are small. Imperfect pulse performance at low rf fields is caused mainly by chemical shifts and field inhomogeneities which cause the Larmor frequency of the spins to differ from site to site in the sample. If the electronic shielding constant for a site is $\sigma^j$, and the applied magnetic field is $B_0$, the Larmor frequency $\omega_0^j$ of that site is given by:

$$\omega_0^j = -\gamma_I B_0(1 - \sigma^j) \tag{4}$$

The *resonance offset* $\Delta\omega^j$ of a set of chemically equivalent spins $I_j$ is equal to the difference between the Larmor frequency and the irradiation frequency:

$$\Delta\omega^j = \omega_0^j - \omega_1 \tag{5}$$

For a sample containing only one chemical site, in a perfectly homogeneous static magnetic field, $\Delta\omega^j$ may be set to zero simply by using an rf $\omega_1$ exactly equal to the chemically-shifted Larmor frequency $\omega_0^j$. However, when the sample contains many different chemical sites, or when the static field is inhomogeneous, resonance offset effects are inevitable.

The seriousness of resonance offset effects may be quantified by the dimensionless parameter $\Delta\omega^j/\Omega_1^0$ which will be called the *relative resonance offset*. For high-resolution proton spectroscopy, the magnitude of the relative offset is typically less than 0.1. For decoupling experiments, and for composite pulses on nuclei with larger chemical shift ranges, relative offsets of 1.0 or more are common.

The resonance offsets $\Delta\omega^j$ may have either algebraic sign, depending on whether the Larmor frequency is higher or lower than the irradiation frequency. For a conventionally presented spectrum of nuclei with a positive magnetogyric ratio such as $^1$H or $^{13}$C, spins with positive $\Delta\omega^j$ appear on the right-hand side of the spectrum. (Remember that the Larmor frequency $\omega_0^j$ and irradiation frequency $\omega_1$ are close to $-\gamma_I B_0$ and are therefore negative.)

#### *3.2.2 Anisotropic Liquids and Solids*

In anisotropic systems, the situation is more complicated as there are many spin interactions large enough to compete with the applied rf field. For spins $I \geqslant 1$, quadrupolar interactions are usually dominant. For $^1$H spins in solids, on the other hand, through-space dipole–dipole interactions are large and produce imperfect pulse performance. For dilute spin-$\frac{1}{2}$ nuclei like $^{13}$C and $^{15}$N, chemical shifts often dominate and the situation is similar to that in isotropic liquids, although the magnitude of the interactions is larger.

The anisotropic case is examined in Section 6 of this article. In most of the following discussion, isotropic liquid phase is assumed and resonance offset effects quantified by the parameter $\Delta\omega^j/\Omega_1^0$.

### 3.3 Other Pulse Imperfections

There are a number of other common pulse imperfections, such as errors in the profile of the pulse in time, errors or instability in the rf phase, and induced fields associated with coupling of the nuclear spin magnetization to the resonant detection coil (see ***Concentrated Solution Effects***). Generally speaking these errors are left uncompensated by composite pulses, although there are exceptions. In particular, composite pulses always assume highly accurate and stable rf phases. Fortunately, digital electronic synthesis of the rf signals generally ensures precise phases in modern instruments.

## 4 AN EXAMPLE OF ERROR COMPENSATION: THE COMPOSITE PULSE $90_{90}180_0 90_{90}$

To introduce the concept of error compensation, consider one of the common tasks of a 180° pulse, namely the sign inversion of the $z$ component of spin angular momentum. This corresponds to an exchange of spin state populations and is often exploited for measuring relaxation time constants (see ***Relaxation: An Introduction***).

### 4.1 Single Pulse Propagator

Consider a single rectangular pulse of nominal flip angle $\beta_p^0$ and phase $\phi_p$. If the rf field is much larger than the spin–spin couplings, and $\beta_p^0$ is not extremely large, then the pulse duration is short on the timescale of spin–spin couplings and the individual spin states undergo a simple rotation in three-dimensional space. The quantum states $|\psi\rangle^j$ of spins $I_j$ before and after a pulse $p$ are related by

$$|\psi\rangle^j_{\text{after}} = \hat{U}_p^j |\psi\rangle^j_{\text{before}} \tag{6}$$

where $\hat{U}_p^j$ is the rotating frame pulse *propagator* for spins $I_j$, given by

$$\hat{U}_p^j = \exp\{-i\xi_p^j \hat{\boldsymbol{I}}_j \cdot \boldsymbol{n}_p^j\} \tag{7}$$

$\xi_p^j$ is the rotation angle of spins $I_j$ during pulse $p$, and $\boldsymbol{n}_p^j$ is the rotation axis.

For an *ideal pulse* of nominal flip angle $\beta_p^0$ and phase $\phi_p$, the rotation angle is $\xi_p^j = \beta_p^0$, and the rotation axis is $\boldsymbol{n}_p^j = \boldsymbol{e}_x \cos\phi_p + \boldsymbol{e}_y \sin\phi_p$, where $\boldsymbol{e}_x$ and $\mathbf{e}_y$ are unit vectors along the $x$ and $y$ axes. If there are finite resonance offset effects or rf amplitude errors, on the other hand, the rotation parameters are

$$\xi_p^j = \beta_p^0 \sqrt{\frac{(\Omega_1)^2 + (\Delta\omega^j)^2}{(\Omega_1^0)^2}} \tag{8}$$

$$\boldsymbol{n}_p^j = \boldsymbol{e}_z \cos\theta^j + \boldsymbol{e}_x \sin\theta^j \cos\phi_p + \boldsymbol{e}_y \sin\theta^j \sin\phi_p \tag{9}$$

where the angle $\theta^j$ is

$$\tan\theta^j = \Omega_1/\Delta\omega^j \tag{10}$$

### 4.2 Single $180_0$ Pulse

Consider now the specific case of a $180_0$ pulse, i.e. $\beta_p^0 = \pi$ and $\phi_p = 0$. For small offsets $\Delta\omega^j/\Omega_1^0$, the propagator is simply

$$\hat{U}_p^j \simeq \exp\{-i\xi_p^j \hat{I}_{jx}\} \tag{11}$$

with

$$\xi_p^j = \pi\Omega_1/\Omega_1^0 \tag{12}$$

indicating that the spin angular momentum turns through an angle $\xi_p^j$ about the $x$ axis of the rotating reference frame. Depending on the rf field $\Omega_1$, this angle can be either smaller or greater than the nominal flip angle $\beta_p^0 = \pi$.

The transformation of $z$ angular momentum by an imperfect $180_0$ pulse is readily understood geometrically. An ensemble of spins $I_j$ with finite polarization along the $z$ axis has a spin density operator $\hat{\sigma}_{\text{before}} = \hat{I}_{jz}$ (inessential constants being omitted). This can be represented as an angular momentum vector along the $z$ axis of the rotating reference frame [Figure 1(a)]. After the pulse the density operator is

$$\begin{aligned}\hat{\sigma}_{\text{after}} &= \hat{U}_p^j \hat{I}_{jz} \hat{U}_p^{j\dagger} \\ &= \hat{I}_{jz}\cos\xi_p^j - \hat{I}_{jy}\sin\xi_p^j\end{aligned} \tag{13}$$

This can be understood as a rotation of the angular momentum of the spin ensemble around the $x$ axis through an angle $\xi_p^j$. For nominal rf fields, $\xi_p^j = \pi$ and the spin angular momentum is along the $-z$ axis after the pulse [Figure 1(b)]. For rf fields larger than the nominal [Figure 1(c)], the vector 'overshoots' the $-z$ axis, and for weak rf fields, the vector falls short [Figure 1(d)]. The transformed $z$ angular momentum of spins $I_j$, given by the parameter

$$\begin{aligned}R_{zz}^j &= \text{Tr}\{\hat{U}_p^j \hat{I}_{jz} \hat{U}_p^{j\dagger} \hat{I}_{jz}\}/\text{Tr}\{\hat{I}_{jz}^2\} \\ &= \cos\xi_p^j\end{aligned} \tag{14}$$

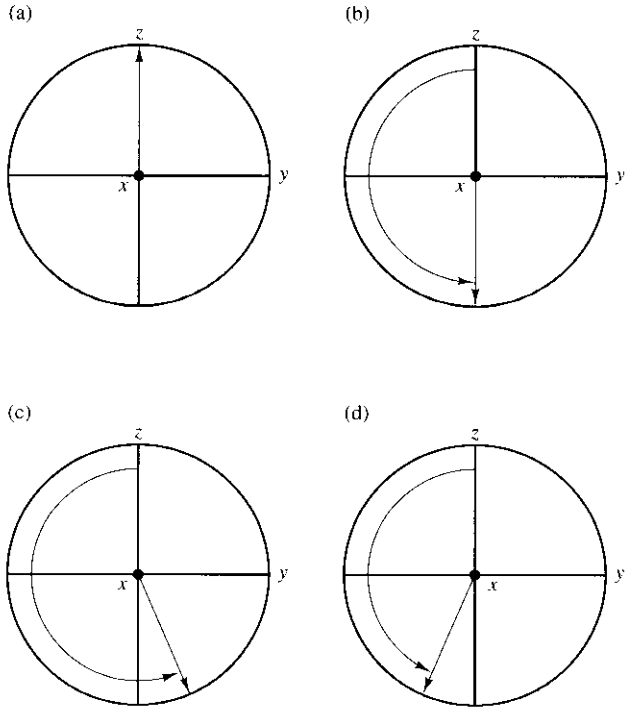


**Figure 1** Effect of an imperfect rf field on a $180_0$ pulse. (a) The equilibrium spin magnetization is represented as a unit vector along the $z$ axis of the rotating reference frame. (b) For nominal rf fields ($\Omega_1 = \Omega_1^0$), the magnetization vector rotates through 180° around the $x$ axis, ending up exactly at the $-z$ axis. (c) For rf fields stronger than the nominal, the magnetization vector overshoots the $-z$ axis. (d) For rf fields weaker than the nominal, the vector falls short of the $-z$ axis. In both cases, the $z$ component of the final vector is larger than $-1$

is equal to $-1$ for an ideal $180_0$ pulse, but is larger than $-1$ if the pulse is imperfect [Figure 2(a)]. For small rf field errors, the transformed $z$ angular momentum is

$$R_{zz}^j \simeq -1 + \tfrac{1}{2}\pi^2 \left(\frac{\Omega_1 - \Omega_1^0}{\Omega_1^0}\right)^2 \tag{15}$$

i.e. it is quadratically dependent on the rf error. In practice this means that the degree of spin population inversion is spatially dependent, with detrimental experimental consequences.

### 4.3 Composite Pulse $90_{90}180_0 90_{90}$

The imperfect transformation of $z$ angular momentum may be corrected[9] by using a composite pulse $90_{90}180_0 90_{90}$ as illustrated in Figure 3. The trajectories of the tips of a family of vectors, all starting out along the $z$ axis, are tracked out during the pulse sequence. The vectors in the family correspond to different rf field values; to simplify the picture, all represent rf fields weaker than the nominal.

During the first $90_{90}$ element, all vectors rotate around the $y$ axis, starting at the $z$ axis and turning towards the $x$ axis. An ideal $90_{90}$ pulse would take them exactly to the $x$ axis, but, as the fields are weak, they fall short. The next $180_0$ element rotates these vectors around the $x$ axis. After this element, the vectors still lie approximately in the $xz$ plane, but they now lie in the southern hemisphere of the unit sphere. Indeed, the tips

For References see p. 1410

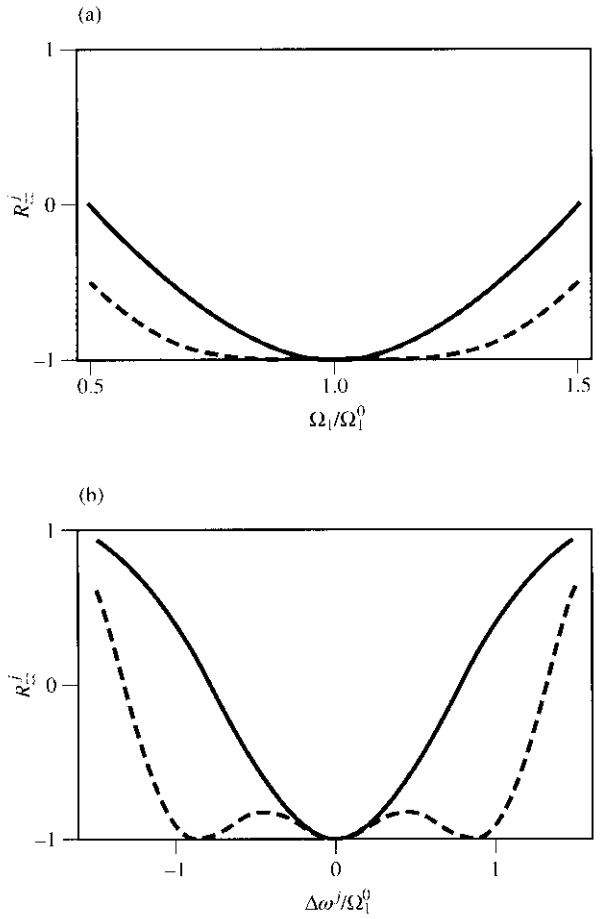


**Figure 2** Transformation parameters of $z$ angular momentum $R^j_{zz}$ for a single $180_0$ pulse (——), and a composite $90_{90}180_0 90_{90}$ pulse (– – –). (a) Dependence of $R^j_{zz}$ on the rf field $\Omega_1/\Omega_1^0$. (b) Dependence of $R^j_{zz}$ on the relative resonance offset $\Delta\omega^j/\Omega_1^0$

of the vectors after the first and second pulses are related as approximate mirror images in the $xy$ plane. The last $90_{90}$ element again rotates the vectors around the $y$ axis, through exactly the same angle as the first element. The error compensation works as follows; just those vectors which lag the most after the first pulse are helped the most by the second pulse, so that they don't have as far to go during the last pulse. On the other hand, if the rf field is close to the nominal, the vectors are already taken nearly to the $x$ axis by the first pulse, so that they are almost unaffected by the second pulse. Again they are in the right position to be taken to the $-z$ axis by the last pulse. Hence the angular momentum vectors for spins in a range of rf fields concentrate near the $-z$ axis at the end of the sequence. A plot of $R^j_{zz}$ against relative rf field $\Omega_1/\Omega_1^0$ for the composite pulse $90_{90}180_0 90_{90}$ is shown by the dashed line in Figure 2(a).

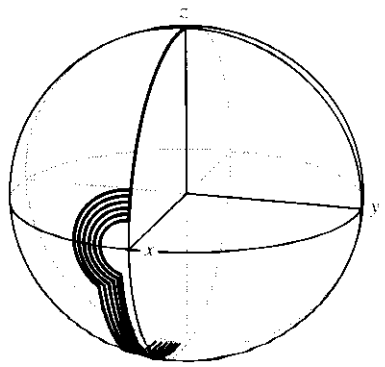


**Figure 3** Geometrical mechanism of rf field compensation for the composite pulse $90_{90}180_0 90_{90}$

An accurate analysis of the sequence $90_{90}180_0 90_{90}$ shows[10] that for small resonance offsets the transformed $z$ angular momentum is given by

$$R^j_{zz} = \cos\left\{2\arccos\left[\cos^2\left(\frac{\pi\Omega_1}{2\Omega_1^0}\right)\right]\right\} \tag{16}$$

For small rf field errors this can be approximated as

$$R^j_{zz} \simeq -1 + \tfrac{1}{8}\pi^4\left(\frac{\Omega_1 - \Omega_1^0}{\Omega_1^0}\right)^4 \tag{17}$$

The transformation of $z$ magnetization is sensitive only to the fourth order in rf field error.

It happens that $90_{90}180_0 90_{90}$ also gives a rather good compensation for resonance offsets, as long as the rf field intensity is close to the nominal. A simulation of $R^j_{zz}$ against resonance offset $\Delta\omega^j/\Omega_1^0$, in the case of an exactly set rf field $\Omega_1 = \Omega_1^0$, is shown in Figure 2(b). The compensation of offset is not very exact, but quite broadband, giving fair inversion of $z$ angular momentum for all offsets between $-1.0 \leqslant \Delta\omega^j/\Omega_1^0 \leqslant 1.0$.

A picture of what happens when both offset and rf error are introduced at the same time is given in Figure 4(b). This shows

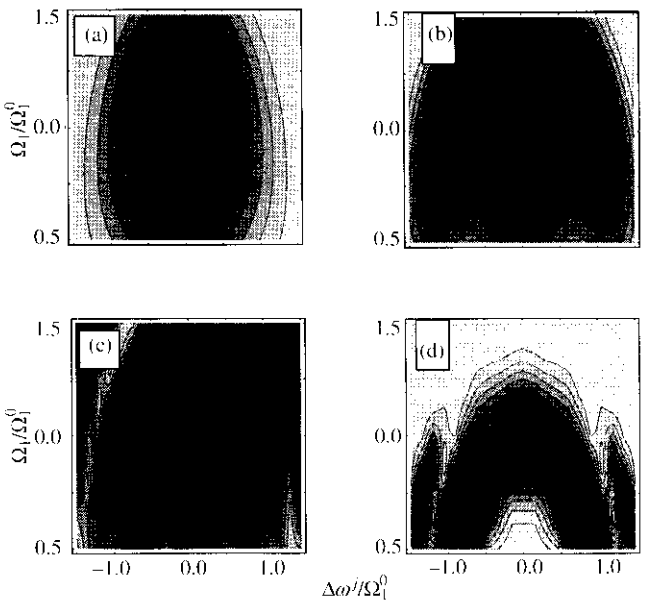


**Figure 4** Contour plots of the parameter $R^j_{zz}$ as a function of rf field $\Omega_1/\Omega_1^0$ and resonance offset $\Delta\omega^j/\Omega_1^0$ for four different pulse sequences. Inside the darkest region, the parameter $R^j_{zz}$ is less than $-0.98$. Increasingly bright regions are delimited by contours at $\{-0.95, -0.9, -0.8, -0.6, -0.4, \ldots\}$. (a) Single pulse $180_0$. (b) Composite pulse $90_{90}180_0 90_{90}$. (c) Composite pulse $270_{180}360_0 90_{90}270_{270}360_0 90_0$. (d) Composite pulse $180_{30}180_{205}180_{230}180_{85}180_0 180_{85}180_{230}180_{205}180_{30}$

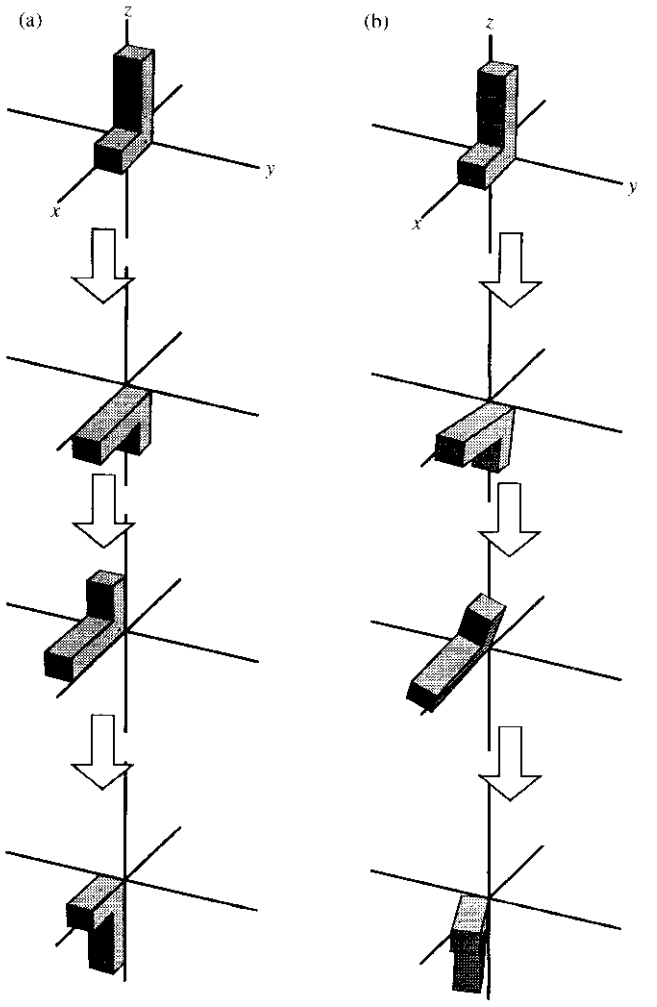


**Figure 5** Transformations of a three-dimensional object by a succession of three rotations. (a) A 90° rotation about the $y$ axis, followed by a 180° rotation about the $x$ axis, followed by a 90° rotation about the $y$ axis. (b) A 80° rotation about the $y$ axis, followed by a 160° rotation about the $x$ axis, followed by a 80° rotation about the $y$ axis

a contour plot of $R_{zz}^{j}$ against resonance offset $\Delta\omega^{j}/\Omega_1^0$ (horizontal) and rf field $\Omega_1/\Omega_1^0$ (vertical). The darkest portions of the plot are regions of excellent population inversion ($R_{zz}^{j} \leqslant -0.98$). These regions are far more extensive for $90_{90}180_{0}90_{90}$ than for a single pulse $180_0$ [Figure 2(a)]. However, the sequence $90_{90}180_{0}90_{90}$ cannot strictly be said to compensate for *simultaneous* resonance offset and rf field errors. There is trouble if the rf field is weak at the same time as there is a moderate resonance offset. For truly simultaneous compensation, one must use more complicated sequences, such as

$$270_{180}360_{0}90_{90}270_{270}360_{90}90_{0} \tag{18}$$

whose performance is illustrated in Figure 4(c).[11]

The above analysis considered only the $z$ component of spin angular momentum. In general, other angular momentum components are also important. Figure 5 illustrates the subtleties which arise when composite pulses are applied to general states of the spin ensemble. The spin density operator is represented not as a vector but as a full three-dimensional object with low symmetry, here a simple L shape.

In Figure 5(a) the L shape is subjected to a sequence of three rotations, a 90° rotation around the $y$ axis, followed by a 180° rotation around the $x$ axis, and a 90° rotation around the $y$ axis again. These three rotations may be shown to be equivalent to a single rotation, through 180° around the $x$ axis, as shown by the final position in Figure 5(a).[12] The composite pulse $90_{90}180_{0}90_{90}$ is equivalent to a single $180_0$, if all pulses are ideal.

Figure 5(b) illustrates the behavior of the composite pulse if the rf field is somewhat weaker than nominal. After the three mis-set rotations, the long arm of the L is taken almost exactly to the $-z$ axis, as expected from Figure 3. However, the L shape is also rotated *around* the $z$ axis, as can be seen by comparing the final positions in Figures 5(a) and (b). In the language of nuclear spin dynamics, the compensated population inversion is accompanied by a *phase shift* of the spin coherences. Such induced *phase distortions* are a common feature of most composite pulses, and must carefully be taken into account in general applications.

## 5 COMPOSITE PULSES: SPIN COUPLINGS IGNORED

The response of a general spin system to a composite pulse raises complex issues. Fortunately, the treatment is greatly simplified if the composite pulse is very short compared with the spin–spin coupling constants. Under this approximation, all rf pulses induce simple three-dimensional rotations of the individual spin angular momenta. Such composite pulses can be considered manifestations of the three-dimensional rotation group, and are amenable to geometric representation.

This type of composite pulse only works properly if it is short compared with the timescale set by spin–spin couplings and spin relaxation. This condition is usually readily satisfied in isotropic liquids. Breakdown of this assumption eventually sets a limit on the length of usable sequences.

This restriction should not be taken to imply that such composite pulses can only be applied to systems without spin–spin couplings. The point is merely that the couplings can be ignored *during* the composite pulse. The spin–spin couplings can still be active during the much longer periods *between* the pulses.

A smaller group of composite pulses (discussed in Section 6) takes into account explicitly the spin couplings during the pulse. The dynamics of the spins cannot then be described as rotations in a three-dimensional space.

### 5.1 Composite Pulse Propagator

Consider a composite pulse with $n$ pulse elements, applied to a system of $N$ coupled spins. If the spin–spin couplings are neglected, the overall propagator $\hat{U}$ of the entire spin system can be factorized into a product of individual propagators $\hat{U}^{j}$, one for each spin:

$$\hat{U} \approx \hat{U}^{1}\hat{U}^{2}\cdots\hat{U}^{N} \tag{19}$$

For References see p. 1410

**Table 1** Variable Rotation Composite 90° Pulses[a]

| Sequence | Ref. | rf field range $(\Omega_1/\Omega_1^0)^b$ | Offset range $(\Delta\omega^j/\Omega_1^0)^c$ |
|---|---|---|---|
| $90_0$ | – | {0.89, 1.11} | {−0.92, 0.92} |
| $90_0 90_{90}$ | 18 | **{0.73, 1.27}** | *{−0.10, 0.10}* |
| $90_0 180_{120}$ | 19 | **{0.62, 1.37}** | *{−0.13, 0.10}* |
| $180_{97.2} 360_{291.5} 180_{97.2} 90_0$ | 15 | **{0.58, 1.42}** | *{−0.88, 0.36}* |
| $180_0 360_{180} 180_0 270_{180} 90_{90}$ | 42 | **{0.58, 1.42}** | **{−1.24, 1.24}** |

[a]Bandwidths which are extended with respect to a single 90° pulse are in bold type. Bandwidths which are contracted with respect to a single 90° pulse are in italics.
[b]The range of rf field values for which the angle $\bar{\beta}^j$ is between 80° and 100°, at zero resonance offset.
[c]The range of offset values for which the angle $\bar{\beta}^j$ is between 80° and 100°, at nominal rf field.

The individual spin propagators $\hat{U}^j$ all commute, so equation (19) can be written in any order. Each overall spin propagator $\hat{U}^j$ is, in turn, a product of spin rotations $\hat{U}_p^j$ corresponding to the individual pulses $p$:

$$\hat{U}^j = \hat{U}_n^j \cdots \hat{U}_2^j \hat{U}_1^j \tag{20}$$

$\hat{U}_p^j$ is given in equation (7). The operators $\hat{U}_p^j$ do not commute, so the product must be written in strict chronological order from right to left.

Since any product of rotations is another rotation, the overall composite pulse propagator for each individual spin $I_j$ is also a rotation operator, and can be written in the form

$$\hat{U}^j = \exp\{-i\bar{\xi}^j \hat{\boldsymbol{I}}_j \cdot \bar{\boldsymbol{n}}^j\} \tag{21}$$

where $\bar{\xi}^j$ is the overall rotation angle, and $\bar{\boldsymbol{n}}^j$ is the overall rotation axis.

There is another way of writing equation (21), which brings out more clearly the 'phase-distortion' properties of the composite pulse. Any rotation can be expressed as three consecutive rotations, about the $z$ axis, the $y$ axis, and the $z$ axis again. The composite pulse propagator can therefore be written

$$\hat{U}^j = \exp\{-i\bar{\gamma}^j \hat{I}_{jz}\} \exp\{-i\bar{\beta}^j \hat{I}_{jy}\} \exp\{-i\bar{\alpha}^j \hat{I}_{jz}\} \tag{22}$$

where the three angles $\{\bar{\alpha}^j, \bar{\beta}^j, \bar{\gamma}^j\}$ are called the *Euler angles* for the overall rotation.[13] In general, the Euler angles depend on the parameters $\Omega_1/\Omega_1^0$ and $\Delta\omega^j/\Omega_1^0$, and are different for each set of spins $I_j$.

## 5.2 Classification of Composite Pulses

The properties of composite pulses are defined by the dependence of the three Euler angles $\{\bar{\alpha}^j, \bar{\beta}^j, \bar{\gamma}^j\}$ on the imperfection parameters $\Delta\omega^j/\Omega_1^0$ and $\Omega_1/\Omega_1^0$.

The central angle $\bar{\beta}^j$ is the most important. If $\bar{\beta}^j$ is close to some angle $\Theta$, the composite pulse behaves 'like' an ideal pulse of nominal flip angle $\Theta$. The composite pulse is then called a *composite* $\Theta$ *pulse*. For example, $90_{90}180_0 90_{90}$ is a composite 180° pulse since $\bar{\beta}^j$ is close to 180° for small values of $\Delta\omega^j/\Omega_1^0$ and $\Omega_1/\Omega_1^0$.

### 5.2.1 *Broadband Composite Pulses*

Often, the composite pulse is designed such that $\bar{\beta}^j$ remains close to some value $\Theta$ over a range of rf field or resonance offset which is larger than for a single pulse. The composite pulse is then called a *broadband composite* $\Theta$ *pulse*.

The range of rf field or resonance offset for which $\bar{\beta}^j$ is 'close' to $\Theta$ is called the *compensation bandwidth*. The compensation bandwidths of some selected composite pulses are given in Tables 1 and 2. The tabulated figures indicate the

**Table 2** Variable Rotation Composite 180° Pulses[a]

| Sequence | Ref. | rf field range $(\Omega_1/\Omega_1^0)^b$ | Offset range $(\Delta\omega^j/\Omega_1^0)^c$ |
|---|---|---|---|
| $180_0$ | – | {0.94, 1.06} | {−0.08, 0.08} |
| $90_{90} 180_0 90_{90}$ | 9 | **{0.81, 1.19}** | {−0.09, 0.09} |
| $90_0 360_{120} 90_0$ | 19 | **{0.71, 1.29}** | {−0.08, 0.08} |
| $180_{120} 180_{240} 180_{120}$ | 33 | **{0.71, 1.29}** | *{−0.05, 0.05}* |
| $180_{104.5} 360_{313.4} 180_{104.5} 180_0$ | 15 | **{0.69, 1.31}** | {−0.09, 0.09} |
| $90_0 225_{180} 315_0$ | 29 | {0.94, 1.06} | **{−0.68, 0.68}** |
| $158_{180} 171.2_0 342.8_{180} 145.5_0 81.2_{180} 85.3_0$ | 28 | {0.94, 1.06} | **{−1.50, 1.50}** |
| $90_0 240_{90} 90_0$ | 18 | **{0.67, 1.09}** | **{−0.52, 0.52}** |
| $270_{180} 360_0 90_{90} 270_{270} 360_{90} 90_0$ | 11 | **{0.72, 1.28}** | **{−0.45, 0.50}** |
| $180_0 180_0 180_{120} 180_{60} 180_{120} 180_0 180_0 180_{120} 180_{60} 180_{120}$ $180_{120} 180_{120} 180_{240} 180_{180} 180_{240} 180_{60} 180_{60} 180_{180} 180_{120}$ $180_{180} 180_{120} 180_{120} 180_{240} 180_{180} 180_{240}$ | 34 | **{0.68, 1.33}** | **{−0.76, 0.95}** |

[a]Bandwidths which are extended with respect to a single 180° pulse are in bold type. Bandwidths which are contracted with respect to a single 180° pulse are in italics.
[b]The range of rf field values for which the angle $\bar{\beta}^j$ is between 170° and 190°, at zero resonance offset.
[c]The range of offset values for which the angle $\bar{\beta}^j$ is between 170° and 190°, at nominal rf field.

**Table 3** Constant Rotation Composite 90° Pulses[a]

| Sequence | Ref. | rf field range $(\Omega_1/\Omega_1^0)^b$ | Offset range $(\Delta\omega^j/\Omega_1^0)^c$ |
|---|---|---|---|
| $90_0$ | – | {0.89, 1.11} | {−0.13, 0.13} |
| $385_0320_{180}25_0$ | 25 | {0.89, 1.11} | **{−0.30, 0.30}** |
| $113_{180}316_0113_{180}$ | 27 | {0.89, 1.11} | **{−0.26, 0.26}** |
| $24_0152_{180}346_0152_{180}24_0$ | 27 | {0.89, 1.11} | **{−0.40, 0.40}** |
| $119_{180}183_0211_{180}384_0211_{180}183_0119_{180}$ | 27 | {0.89, 1.11} | **{−0.83, 0.83}** |
| $180_{97.2}360_{291.5}180_{97.2}90_0$ | 15 | **{0.59, 1.41}** | {−0.13, 0.13} |

[a]Bandwidths which are extended with respect to a single 90° pulse are in bold type.
[b]The range of rf field values for which the angle $\bar{\xi}_\Delta^j$ is less than 10°, at zero resonance offset.
[c]The range of offset values for which the angle $\bar{\xi}_\Delta^j$ is less than 10°, at nominal rf field.

range of $\Delta\omega^j/\Omega_1^0$ and $\Omega_1/\Omega_1^0$ within which $\bar{\beta}^j$ is within 10° of the flip angle $\Theta$. For example, for the composite pulse $90_{90}180_0 90_{90}$, the angle $\bar{\beta}^j$ is between 170° and 190° for all values of rf field in the range $0.81 \leqslant \Omega_1/\Omega_1^0 \leqslant 1.19$, if the resonance offset is zero. Similarly, $\bar{\beta}^j$ is between 170° and 190° for all values of resonance offset in the range $-0.09 \leqslant \Delta\omega^j/\Omega_1^0 \leqslant 0.09$, providing the rf field is nominal. Parameter ranges which are extended with respect to a single rf pulse are indicated in bold type. Those which are more restricted than for a single pulse are in italics. For example, the sequence $180_{120}180_{240}180_{120}$ tolerates a wider range of rf field strengths than a single $180_0$ pulse, but only if the resonance offset is kept within stringent limits.

Since $R_{zz}^j$ is equal to $\cos\beta^j$, the quoted bandwidths also apply to the corresponding transformations of $z$ angular momentum. For composite 180° pulses, $R_{zz}^j$ is less than −0.984 within the quoted bandwidths; for composite 90° pulses, $R_{zz}^j$ is between −0.17 and +0.17 over the tabulated compensation bands.

This bandwidth definition does not yet say anything about the angles $\bar{\alpha}^j$ and $\bar{\gamma}^j$. The behavior of these angles introduces further nuances:

1. For *variable rotation composite pulses*, the Euler angles $\bar{\alpha}^j$ and $\gamma^j$ are unconstrained, and may vary arbitarily within the compensation band.
2. For *constant rotation composite pulses*, the only variations in $\alpha^j$ and $\bar{\gamma}^j$ over the compensation band keep the overall rotation operator $\hat{U}^j$ close to that generated by an ideal $\Theta_0$ pulse.[4]

In Tables 3 and 4, some constant rotation composite pulses are listed, together with the ranges of $\Delta\omega^j/\Omega_1^0$ and $\Omega_1/\Omega_1^0$ for which they provide a rotation close to the ideal. The compensation range of such composite pulses is more difficult to define than for variable rotation composite pulses, since all three Euler angles are involved. The tabulated constant rotation bandwidths are based upon the values of the angle $\bar{\xi}_\Delta^j$, defined by the equation

$$\hat{U}^j - \exp\{-i\Theta\hat{I}_{jx}\}\exp\{-i\bar{\xi}_\Delta^j \hat{\boldsymbol{I}}_j \cdot \boldsymbol{n}_\Delta^j\} \tag{23}$$

where $\hat{U}^j$ is given by equation (21) and $\boldsymbol{n}^j{}_\Delta$ is a unit vector. $\xi^j{}_\Delta$ can be interpreted as the 'deviation angle' between the actual rotation $\hat{U}^j$ and the desired ideal rotation. If the rotation is already ideal, $\xi^j{}_\Delta$ is equal to zero. In terms of the Euler angles, it can be shown that $\bar{\xi}^j{}_\Delta$ is given by

$$\begin{aligned}\cos(\bar{\xi}_\Delta^j/2) = {} & \cos(\bar{\beta}^j/2)\cos(\Theta/2)\cos\left(\frac{\alpha^j + \gamma^j}{2}\right) \\ & + \sin(\bar{\beta}^j/2)\sin(\Theta/2)\sin\left(\frac{\alpha^j - \bar{\gamma}^j}{2}\right)\end{aligned} \tag{24}$$

The tabulated constant rotation bandwidths indicate the range of $\Delta\omega^j/\Omega_1^0$ and $\Omega_1/\Omega_1^0$ for which the 'deviation angle' $\bar{\xi}_\Delta^j$ is always less than 10°. Within these parameter ranges the composite pulses may be used to replace the single pulse, independent of the experimental context.

The distinction between the different types of composite pulse is illustrated in Figure 6. This shows the dependence of

**Table 4** Constant Rotation Composite 180° Pulses[a]

| Sequence | Ref. | rf field range $(\Omega_1/\Omega_1^0)^b$ | Offset range $(\Delta\omega^j/\Omega_1^0)^c$ |
|---|---|---|---|
| $180_0$ | – | {0.94, 1.06} | {−0.09, 0.09} |
| $180_{120}180_{240}180_{120}$ | 33 | **{0.80, 1.20}** | *{−0.05, 0.05}* |
| $180_{104.5}360_{313.4}180_{104.5}180_0$ | 15 | **{0.69, 1.31}** | {−0.09, 0.09} |
| $59_{180}298_059_{180}$ | 27 | {0.94, 1.06} | **{−0.23, 0.23}** |
| $58_0140_{180}344_0140_{180}58_0$ | 27 | {0.94, 1.06} | **{−0.39, 0.39}** |
| $27_099_{180}180_0211_{180}386_0211_{180}180_099_{180}27_0$ | 27 | {0.94, 1.06} | **{−0.86, 0.86}** |
| $180_0180_0180_{120}180_{60}180_{120}180_0180_0180_{120}180_{60}$ $180_{120}180_{120}180_{120}180_{240}180_{180}180_{240}180_{60}180_{60}$ $180_{180}180_{120}180_{180}180_{120}180_{120}180_{240}180_{180}180_{240}$ | 34 | **{0.88, 1.12}** | **{−0.48, 0.48}** |

[a]Bandwidths which are extended with respect to a single 180° pulse are in bold type. Bandwidths which are contracted with respect to a single 180° pulse are in italics.
[b]The range of rf field values for which the angle $\bar{\xi}_\Delta^j$ is less than 10°, at zero resonance offset.
[c]The range of offset values for which the angle $\bar{\xi}_\Delta^j$ is less than 10°, at nominal rf field.

For References see p. 1410

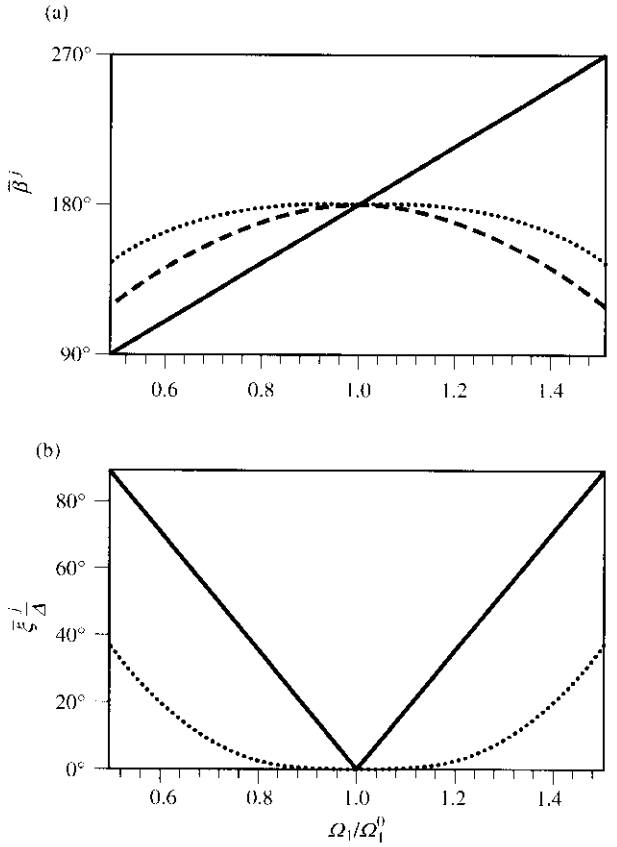


**Figure 6** Performance of the single pulse $180_0$ (——), composite pulse $90_{90}180_0 90_{90}$ (– – –), and composite pulse $180_{104.5}360_{313.4}180_{104.5}180_0$ (· · · ·) as a function of rf field. (a) Euler angle $\bar{\beta}^j$. (b) Deviation angle $\bar{\xi}^j_\Delta$. The curves for the single $180_0$ pulse and composite pulse $90_{90}180_0 90_{90}$ are superimposed in (b)

the angles $\bar{\beta}^j$ and $\bar{\xi}^j_\Delta$ on the rf field $\Omega_1/\Omega_1^0$, for the variable rotation composite pulse $90_{90}180_0 90_{90}$ and the constant rotation sequence $180_{104.5}360_{313.4}180_{104.5}180_0$.[15] In both cases, $\bar{\beta}^j$ is kept close to 180° over a range of rf fields, but $\bar{\xi}^j_\Delta$ is kept low only for the second sequence. The sequence $180_{104.5}360_{313.4}180_{104.5}180_0$ behaves similarly to an ideal pulse $180_0$ over the entire compensation band.

### 5.2.2 *Narrowband and Band-Reject Composite Pulses*

For broadband composite pulses, $\bar{\beta}^j$ is kept almost constant over a certain range of rf fields or resonance offsets. This is not the only possible mode of control of $\bar{\beta}^j$. Some other possibilities are:

1. For *narrowband composite pulses*, $\bar{\beta}^j$ is kept close to zero over a wide range of parameters, except for certain special values, where $\bar{\beta}^j$ is close to the nominal flip angle $\Theta$ of the composite pulse. Narrowband composite pulses can be used for selecting NMR signals originating in spatial regions with defined values of the rf field amplitude.
2. A *band-reject composite pulse* resembles a broadband composite pulse except for a 'hole' in the excitation around some special value of rf field or offset frequency, i.e. $\bar{\beta}^j$ is large over a wide range except in a narrow region where it approximates zero. Composite pulses with band-reject characteristics for offset $\Delta\omega^j/\Omega_1^0$ can be used for solvent peak suppression.

Most of this article concerns broadband composite pulses. The other possibilities are treated briefly in Section 5.6.

## 5.3 Coherence Transfer Amplitudes

To appreciate the practical significance of the angles $\bar{\alpha}^j$ and $\bar{\gamma}^j$, consider the case where the composite pulse is applied to a weakly coupled system of $N$ spins, prepared such that the density operator contains coherences $\sigma_{rs}$ between two spin eigenstates $|r\rangle$ and $|s\rangle$. In general, the composite pulse sequence converts this coherence partially to another coherence $\sigma_{tu}$, between eigenstates $|t\rangle$ and $|u\rangle$. The amplitude for this particular coherence transfer process is written $Z_{rs\ tu}$. The manipulation of spin state populations may be handled by taking the case $r = s$ or $t = u$ (see ***Molecular Motions: $T_1$ Frequency Dispersion in Biological Systems***).

It may be shown that for a composite pulse with a propagator defined by equation (22), within its compensation band, the amplitude for the coherence transfer process is given by

$$Z_{rstu} \simeq \exp\left\{-i\sum_j[(\bar{\gamma}^j + \pi/2)p_j^{(tu)} + (\bar{\alpha}^j - \pi/2)p_j^{(rs)}]\right\}Z^0_{rs\,tu} \quad (25)$$

where $p_j^{(tu)} = m_j^{(t)} - m_j^{(u)}$, $p_j^{(rs)} = m_j^{(r)} - m_j^{(r)}$, and $m_j^{(s)}$ is the $z$ angular momentum of spin $I_j$ in the eigenstate $|s\rangle$ (weak coupling is assumed). $Z^0_{rs\,tu}$ denotes the coherence transfer amplitude for a strong ideal pulse of flip angle $\beta^0$.

The experimental significance of the angles $\bar{\alpha}^j$ and $\bar{\gamma}^j$ depends on the quantum numbers characterizing the coherence transfer process. If only populations are involved ($p_j^{(tu)} = p_j^{(rs)} = 0$), the Euler angles $\bar{\alpha}^j$ and $\bar{\gamma}^j$ may be ignored. If coherences are involved, on the other hand, $\alpha^j$ and $\gamma^j$ must be taken into account.

It would therefore seem advisable to use constant rotation composite pulses whenever spin coherences are involved. However, this is not always the best strategy. Constant rotation composite pulses are often long and have small compensation bandwidths. In many circumstances, variable rotation composite pulses are to be preferred:

1. In heteronuclear experiments, composite pulses applied to one spin species do not affect the phases of coherences associated with a different spin species. For example, variable rotation composite 180° pulses such as $90_{90}180_0 90_{90}$ may be applied to the $I$ spins in order to change the sign of density operator terms such as $\hat{I}_z\hat{S}_x$. Such manipulations are common in two-dimensional heteronuclear shift correlation experiments (see ***Heteronuclear Shift Correlation Spectroscopy***).
2. For some variable rotation composite pulses, the angles $\alpha^j$ and $\bar{\gamma}^j$ are linearly dependent on resonant offset $\Delta\omega^j$. In simple experiments involving only one coherence transfer step, phase distortions can then be removed simply by applying a numerical frequency-dependent phase correction to the spectrum.
3. If a phase cycle is performed so as to select signals arising only from *one single coherence transfer pathway*

(see ***Phase Cycling***), then the angles $\bar{\alpha}^j$ and $\bar{\gamma}^j$ only contribute to a rather harmless overall phase shift of the signal.

4. Even in arbitary experiments involving many coherence transfer steps and many coherence transfer pathways, it is usually possible to choose variable rotation composite pulses such that the phase shifts induced by one composite pulse are cancelled out by the next composite pulse.[7,16,17] A general procedure is described in Section 5.5.

## 5.4 Construction of Broadband Composite Pulses

There is a great variety of theoretical approaches to composite pulse construction. The following summary is superficial.

### 5.4.1 Geometry

The first composite pulse $90_{90}180_{0}90_{90}$ was discovered by the geometrical arguments outlined in Figure 3. This simple method should not be underestimated. It exploits the impressive human faculty of three-dimensional visualization. However, so far, only variable-rotation composite pulses have been derived geometrically. Apart from $90_{90}180_{0}90_{90}$, geometrical reasoning has led to the useful sequences $90_{0}180_{120}$ (an rf-compensated 90° pulse with a large bandwidth) and $90_{0}360_{120}90_{0}$ (a highly rf-compensated 180° pulse).[18–20]

### 5.4.2 Rotation Analysis

Geometrical reasoning may be assisted by mathematical methods such as quaternion algebra[21]. One powerful result is as follows.[10] Suppose a rotation through the angle $\xi_1$ about the axis $\boldsymbol{n}_1$ is followed by a rotation through the angle $\xi_2$ about the axis $\boldsymbol{n}_2$. The two consecutive rotations are equivalent to a single rotation through the angle $\xi_{12}$ about the axis $\boldsymbol{n}_{12}$. It is possible to show that $\xi_{12}$ and $\boldsymbol{n}_{12}$ are given by

$$\left.\begin{aligned} c_{12} &= c_1c_2 - s_1s_2\boldsymbol{n}_1\cdot\boldsymbol{n}_2 \\ s_{12}\boldsymbol{n}_{12} &= s_1c_2\boldsymbol{n}_1 + c_1s_2\boldsymbol{n}_2 - s_1s_2\boldsymbol{n}_1\times\boldsymbol{n}_2 \end{aligned}\right\} \tag{26}$$

where $c_p = \cos(\xi_p/2)$, $s_p = \sin(\xi_p/2)$, $c_{12} = \cos(\xi_{12}/2)$, $s_{12} = \sin(\xi_{12}/2)$.

Using such formulae, it is possible to show, for example, that the Euler angle $\beta^j$ for the composite pulse $90_{90}180_{0}90_{90}$ at resonance offset $\Delta\omega^j = 0$ is given by

$$\cos(\bar{\beta}^j/2) = \cos^2(\pi\Omega_1/2\Omega_1^0) \tag{27}$$

while for the composite pulse $90_{0}360_{120}90_{0}$ the corresponding Euler angle is

$$\cos(\bar{\beta}^j/2) = \cos^3(\pi\Omega_1/2\Omega_1^0) \tag{28}$$

The powers of the cosine function on the right-hand sides of these equations indicate an increasing degree of compensation.

Such results are useful for understanding the response of existing composite pulses but have not yet proved very useful for the design of original sequences.

### 5.4.3 Coherent Averaging Theory

Coherent averaging theory is a form of dynamic perturbation theory, frequently used in multiple pulse sequence development (see ***Average Hamiltonian Theory***; ***Line Narrowing Methods in Solids***). (In the present context, coherent averaging theory writes the 'difference rotation' of equation (23) as a convergent series:

$$\bar{\xi}_\Delta^j\hat{\boldsymbol{I}}_j\cdot\boldsymbol{n}_\Delta^j = \xi_\Delta^{j(0)}\hat{\boldsymbol{I}}_j\cdot\boldsymbol{n}_\Delta^{j(0)}\hat{\boldsymbol{I}}_j + \bar{\xi}_\Delta^{j(1)}\hat{\boldsymbol{I}}_j\cdot\boldsymbol{n}_\Delta^{j(1)} + \ldots \tag{29}$$

For a given type of imperfection, it is possible to develop simple algebraic equations for the terms $\bar{\xi}_\Delta^{j(k)}$ as functions of the pulse durations and phases. By solving the equations analytically or numerically, pulse sequences are derived for which as many terms $\bar{\xi}_\Delta^{j(k)}$ as possible vanish. The more terms that are removed, the higher the degree of compensation.[15,22–26]

This approach allows the construction of constant rotation composite pulses. One example is the offset-compensated composite 90° pulses $385_{0}320_{180}25_{0}$.[26] A continuous set of offset-compensated constant rotation composite pulses with arbitary flip angle $\Theta$ was derived by exploiting pulse sequence symmetries to reduce the number of simultaneous equations.[27] Two such constant rotation offset-compensated composite pulses are the 180° pulse $59_{180}298_{0}59_{180}$ and the 90° pulse $114.3_{180}318.6_{0}114.3_{180}$.[27]

A continuous set of rf-compensated constant rotation composite pulses has also been found.[15] An rf-compensated rotation with $\bar{\beta}^j \simeq \Theta$ is generated by the sequence $180_{\phi_1}360_{\phi_2}180_{\phi_1}\Theta_0$ where $\phi_1 = \arccos(-\Theta/4\pi)$ and $\phi_2 = 3\phi_1$. Two examples are the broadband 180° pulse $180_{104.5}360_{313.4}180_{104.5}180_{0}$ and the broadband 90° pulse $180_{97.2}360_{291.5}180_{97.2}90_{0}$.

### 5.4.4 Numerical Optimization

It is also feasible to find composite pulses by fairly straightforward numerical optimization methods. The multidimensional space of pulse durations and pulse phases is searched until a sequence with the required properties is found.[8,27–31] Efficient optimization algorithms such as simulated annealing are often helpful.[30,31] Pulse sequence symmetry may be used to reduce the number of independent variables.

Another variant is to extend the bandwidth of an existing composite pulse by adding small extra pulses and optimizing numerically. This can be repeated many times. An example is the composite 180° pulse $158.0_{0}$ $171.2_{180}$ $342.8_{0}$ $145.5_{180}$ $81.2_{0}$ $85.3_{180}$ which has $\bar{\beta}^j \simeq \pi$ over a wide range $-1.5 \leqslant \Delta\omega^j/\Omega_1^0 \leqslant 1.5$.[28] A different starting point is provided by analytical results for *smooth* rf waveforms (see ***Shaped Pulses***). The composite 180° pulse $64_{232}$ $122_{96}$ $310_{0}$ $122_{96}$ $64_{232}$ was derived this way.[32] Wide bandwidth variable rotation composite pulses may be constructed particularly rapidly by allowing the rf frequencies $\omega_1$ of subsequent pulses to be different.[8]

### 5.4.5 Iterative Expansion

Highly compensated sequences require very many pulses. It is very difficult to find such sequences by theoretical techniques such as coherent averaging theory (since the number of simultaneous equations becomes very large) or by numerical optimization (which eventually resembles searching for a

For References see p. 1410

needle in a haystack). A complementary approach is *iterative expansion*.[23,33–39] This defines an optimization procedure which (given a suitable starting point) leads inexorably to a sequence with the desired properties. The drawback is that the process is inefficient, often producing extremely long pulse sequences with moderate bandwidths. However, they can be very accurate.

Iterative expansion starts with some pulse sequence $\mathbb{S}^{(0)}$ whose properties are close to those desired. The sequence is duplicated a small number of times $Q$. Each of the $Q$ clones is subjected to a different 'mutation' which preserves its length. Two common transformations are to change the phase, or to permute an element from the beginning to the end. The $Q$ mutations $\{\mathbb{S}_1^{(0)} \ \ldots \ \mathbb{S}_Q^{(0)}\}$ are spliced together to form a sequence $\mathbb{S}^{(1)}$ which is $Q$ times longer than $\mathbb{S}^{(0)}$:

$$\mathbb{S}^{(1)} = \mathbb{S}_1^{(0)}\mathbb{S}_2^{(0)}\cdots\mathbb{S}_Q^{(0)} \tag{30}$$

The properties of the expansion depend on the mutations and their order. In many cases, it is possible to demonstrate that as long as $\mathbb{S}^{(0)}$ performs reasonably well, then $\mathbb{S}^{(1)}$ will perform better. Hence $\mathbb{S}^{(1)}$ can be reinserted in the machinery to derive a sequence $\mathbb{S}^{(2)}$ which performs better still:

$$\mathbb{S}^{(2)} = \mathbb{S}_1^{(1)}\mathbb{S}_2^{(1)}\cdots\mathbb{S}_Q^{(1)} \tag{31}$$

If the original sequence $\mathbb{S}^{(0)}$ has $n$ elements, the sequence $\mathbb{S}^{(M)}$ derived by $M$ stages of expansion has $nQ^M$ elements. Very long sequences with very high performance are rapidly built up.

Some examples of iterative expansion procedures are:

(1) *Cycles* are composite pulses whose overall rotation angles $\{\bar{\alpha},\bar{\beta},\bar{\gamma}\}$ are all very close to zero.[40] They are used for broadband heteronuclear decoupling (see below). Cycles may be constructed by the following twofold iterative expansion.[35,36]

$$\mathbb{S}^{(m+1)} = [\mathbb{E}^{-1}\mathbb{S}^{(m)}\mathbb{E}]_{180}[\mathbb{E}^{-1}\mathbb{S}^{(m)}\mathbb{E}]_0 \tag{32}$$

where $\mathbb{E}$ is an element on the end of $\mathbb{S}^{(m)}$ with $\bar{\beta} \simeq \pi/2$, i.e. a nominal 90° pulse. This procedure consists of chaining together two cyclic permutations of the original sequence with different phases. Ideally, the sense of the cyclic permutation, and order of chaining, is reversed on alternate expansion stages, i.e.

$$\mathbb{S}^{(m+2)} = [\mathbb{E}\mathbb{S}^{(m+1)}\mathbb{E}^{-1}]_0[\mathbb{E}\mathbb{S}^{(m+1)}\mathbb{E}^{-1}]_{180} \tag{33}$$

The accurate broadband cycle WALTZ-16[41] was constructed roughly this way. It is given by

$$\begin{aligned}&270_{180}360_0180_{180}270_090_{180}180_0360_{180}180_0270_{180}-\\&270_0360_{180}180_0270_{180}90_0180_{180}360_0180_{180}270_0-\\&270_0360_{180}180_0270_{180}90_0180_{180}360_0180_{180}270_0-\\&270_{180}360_0180_{180}270_090_{180}180_0360_{180}180_0270_{180}\end{aligned} \tag{34}$$

(2) *Compensated for rf field inhomogeneity 90° pulses* can be constructed by the following twofold expansion:[42]

$$\mathbb{S}^{(m+1)} = [(\mathbb{S}^{(m)})^{rev}]_{270}[\mathbb{S}^{(m)}]_0 \tag{35}$$

The pulse sequence is written in inverse time order, shifted in phase by 270°, and placed next to the original sequence. For example, starting from $\mathbb{S}^{(0)} = 90_0$, we get $\mathbb{S}^{(1)} = 90_{270}90_0$ and $90_{270}90_{180}90_{270}90_0$, and so on. The longer the sequence, the better the rf compensation. This expansion produces variable rotation composite 90° pulses.

3. *Broadband 180° pulses* can be constructed by fivefold expansions, including[33,34]

$$\mathbb{S}^{(m+1)} = [\mathbb{S}^{(m)}]_0[\mathbb{S}^{(m)}]_0[\mathbb{S}^{(m)}]_{120}[\mathbb{S}^{(m)}]_{60}[\mathbb{S}^{(m)}]_{120} \tag{36}$$

This procedure is capable of compensating both resonance offset effects and rf inhomogeneity at the same time or, indeed, any form of pulse imperfection as long as it is reproducible and transforms properly under rf phase shifts. The highly compensated 25-element composite 180° pulse $180_0\ 180_0\ 180_{120}\ 180_{60}\ 180_{120}\ 180_0\ 180_0\ 180_{120}\ 180_{60}\ 180_{120}\ 180_{120}\ 180_{120}\ 180_{240}\ 180_{180}\ 180_{240}\ 180_{60}\ 180_{60}\ 180_{180}\ 180_{120}\ 180_{180}\ 180_{120}\ 180_{120}\ 180_{240}\ 180_{180}\ 180_{240}$ was constructed this way.[33,34] This fivefold expansion procedure gives rise to variable rotation composite 180° pulses.

There is no space here to explain how these iterative expansion schemes work. An illuminating analysis has been given using the mathematical properties of repeated maps.[34]

### 5.5 Global Pulse Sequence Compensation

Variable rotation composite pulses are generally shorter and have wider compensation bandwidths than constant rotation composite pulses. However, they must be used cautiously in experiments involving coherences, since they induce phase shifts according to equation (25).

In weakly coupled spin systems, it is possible to balance the phase shift associated with one composite pulse by an equal and opposite phase shift associated with the following pulse. This requires that all pulses applied to a given spin species are replaced simultaneously by variable rotation composite pulses of compatible construction.

A general method is to replace pulses with flip angle $\Theta$ and phase $\phi$ by composite pulses of the form $[\mathbb{L}]_\phi\ [\mathbb{R}]_{\phi-\Theta}$. Here $\mathbb{R}$ is a composite pulse with flip angle $\bar{\beta}^j \simeq \pi/2$ and $\mathbb{L}$ is a composite pulse with $\bar{\beta}^j \simeq -\pi/2$. The sequence $\mathbb{L}\mathbb{R}$ without any relative phase shift comprises a cycle. For brevity, the composite pulse pair $[\mathbb{L}]_\Phi\ [\mathbb{R}]_\Psi$ is denoted below by $\mathbb{L}_\Phi\mathbb{R}_\Psi$.

For offset compensation, suitable 'left' and 'right' sequences are

$$\left.\begin{aligned}\mathbb{L} &= 180_{180}360_0180_{180}270_0\\ \mathbb{R} &= 90_0\end{aligned}\right\} \tag{37}$$

In this case the Euler angles of the sequence $\mathbb{L}_\phi\mathbb{R}_{\phi\ \Theta}$ are

$$\left.\begin{aligned}\bar{\alpha}^j &\simeq \pi - \frac{\Delta\omega^j}{\Omega_1^0}\cdots\phi\\ \bar{\beta}^j &\simeq \Theta\\ \bar{\gamma}^j &\simeq -\pi + \frac{\Delta\omega^j}{\Omega_1^0} + \phi - \Theta\end{aligned}\right\} \tag{38}$$

In weakly coupled spin systems, the 'extra' $\bar{\alpha}^j$ and $\gamma^j$ rotations commute with the evolution in the interpulse delays. The $\gamma^j$ rotation of one composite pulse can then be cancelled out by the

$\bar{\alpha}^j$ rotation of the following composite pulse, providing the phase of the following pulse and all subsequent ones are shifted by $-\Theta$. These extra phase shifts must be accumulated iteratively throughout the sequence.

For example, a compensated version of the three-pulse sequence

$$(\Theta)_{\phi_1}-\tau-(\Xi)_{\phi_2}-\tau-(\Psi)_{\phi_3}-\ldots \tag{39}$$

is

$$\mathbb{L}_{\phi_1}\left[\mathbb{R}_{\phi_1}-\tau-\mathbb{L}_{\phi_2}\left[\mathbb{R}_{\phi_2}-\tau-\mathbb{L}_{\phi_3}\{\mathbb{R}_{\phi_3}-\ldots\}_{-\Psi}\right]_{-\Xi}\right]_{-\Theta} \tag{40}$$

or, explicitly,

$$\mathbb{L}_{\phi_1}\mathbb{R}_{\phi_1-\Theta}-\tau-\mathbb{L}_{\phi_2-\Theta}\mathbb{R}_{\phi_2-\Theta-\Xi}-\tau-\mathbb{L}_{\phi_3-\Theta-\Xi}\mathbb{R}_{\phi_3-\Theta-\Xi-\Psi}-\ldots \tag{41}$$

This procedure is readily extended to any number of pulses.

For compensation of rf inhomogeneity effects, the composite pulses $\mathbb{L} = 180_{300}90_{180}$ and $\mathbb{R} = 90_0180_{120}$ may be used instead.

The only defect in this scheme, apart from its complexity, is that the $\bar{\gamma}^j$ phase shift induced by the *last* composite pulse is left over at the end of the sequence. For resonance offset compensation this final phase shift is quite harmless. The frequency-dependent phase of the NMR signal is easily corrected by complex multiplication of the spectrum in the usual way. For rf field inhomogeneity, on the other hand, the final phase shift does lead to some signal loss by spatial dispersion of the magnetization vectors.

This type of global pulse sequence compensation has been demonstrated in multiple quantum NMR.[7,16,17]

## 5.6 Nonbroadband Composite Pulses

Error compensation is only one mode of control of the nonlinear spin response. Several applications of composite pulses extend this concept.

### 5.6.1 *Radiofrequency Field Selection*

It is possible to design *narrowband* pulse sequences in which $\bar{\beta}^j$ is very small except for a narrow range of rf field strengths $\Omega_1$. Such pulse sequences do not perturb the spin populations appreciably unless the rf field is close to the nominal value $\Omega_1^0$. It is possible to use this property as a means for *spatial selection* of the NMR signal.[43–48] The pulse sequence is transmitted through an rf excitation coil with a well-defined spatial variation of rf field amplitude $\Omega_1(\boldsymbol{r})$. Only spins located in spatial regions with $\Omega_1 \simeq \Omega_1^0$ contribute strongly to the final NMR signal.

The most widely used composite pulses of this type have $\bar{\beta}^j \simeq \pi$ over a narrow rf field range. Narrowband composite 180° pulses can be engineered by a number of methods, including the threefold iterative expansion scheme.[43]

$$\mathbb{S}^{(m+1)} = [\mathbb{S}^{(m)}]_{240}[\mathbb{S}^{(m)}]_0[\mathbb{S}^{(m)}]_{120} \tag{42}$$

The challenge is to find a pulse sequence with narrowband rf response which is not too adversely affected by resonance offsets. The performance of the composite 180° pulse $180_{30}180_{205}180_{230}180_{85}180_0180_{85}180_{230}180_{205}180_{30}$[48] is illustrated in Figure 4(d). The narrowband selection of rf fields is maintained fairly well within the offset range $-0.3 \leqslant \Delta\omega^j/\Omega_1^0 \leqslant 0.3$.

### 5.6.2 *Frequency-Selective Excitation*

It is also possible to design pulse sequences with a tailored response with respect to the resonance offset $\Delta\omega^j$. For example, pulse sequences may be constructed with $\bar{\beta}^j$ close to 90° over a wide frequency range, except for a narrow 'hole' close to $\Delta\omega^j = 0$. These *band-reject excitation* sequences can be used in the NMR of dilute solutions. Weak off-resonance solute NMR signals may be excited while avoiding the excitation of strong near-resonant signals from abundant solvent spins.

Sequences with this type of frequency-dependent excitation characteristic were available long before the first composite pulse appeared. However, insights from composite pulse design have allowed the construction of sequences which control the *phase* of the excited solute signals, as well as the amplitude. The angles $\dot{\alpha}^j$ and $\bar{\gamma}^j$ may be kept almost constant over the excitation bandwidth. Distortions associated with spectral phase gradients may thereby be avoided.[49–53] The field is discussed further in ***Water Signal Suppression in NMR of Biomolecules***.

### 5.6.3 *Composite z Pulses*

If rf field errors and resonance offset effects are small, the *composite z pulse* $90_{270}\Theta_090_0$ produces an overall rotation defined by the angles $\{\bar{\alpha}^j, \bar{\beta}^j, \bar{\gamma}^j\} \simeq \{\Theta, 0, 0\}$. This represents a rotation of the spin angular momenta through an angle $\Theta$ about the $z$ axis, as is easily verified by rotating any three-dimensional object, on the lines in Figure 5. In high magnetic field this $z$ rotation is equivalent to a phase shift of all *previous* rf pulses by the same angle $\Theta$. It is therefore possible to emulate the effect of arbitary phase shifts on instruments equipped only for phase steps in multiples of 90°.[54,55] This application was important before digital phase shifting became generally available on commercial instruments.

If the rf field is inhomogeneous in space, composite $z$ pulses with very long nominal flip angle $\Theta$ produce a $z$ rotation through a strongly spatially dependent angle $\bar{\alpha}(\boldsymbol{r})$. The effect is similar to a *static field gradient pulse*, except that the inhomogeneity of the rf field, rather than that of the static magnetic field, is involved. Long composite $z$ pulses of this type have been exploited to select signals arising from defined coherence transfer processes, as an alternative to phase cycling.[56] Time can be saved, and the suppression of undesirable signals improved.

# 6 COMPOSITE PULSES: SPIN COUPLINGS INCLUDED

In the applications discussed below, spin couplings are active during the composite pulse, and the dynamics of the spins cannot generally be visualized in three-dimensional space.

For References see p. 1410

## 6.1 Heteronuclear Decoupling in Liquids

One of the most important applications of composite pulses is *broadband heteronuclear decoupling* in liquids (see ***Decoupling Methods***). The NMR signals from one spin species (conventionally denoted as the $S$ spins) is observed at the same time as a second spin species (conventionally the $I$ spins) is irradiated with a long composite pulse sequence. Ideally the $S$ spins evolve independent of the $IS$ spin–spin coupling, even when there is a wide range of chemical shifts of the $I$ spin species.

In isotropic liquids, it is usually a good approximation to ignore the *homonuclear* interactions between the irradiated $I$ spins and take into account only the *heteronuclear* interactions, which are generally an order of magnitude larger. With this assumption, it has been shown that the problem of constructing a broadband decoupling sequence is formally equivalent to the construction of an accurate broadband *cycle* on *isolated* spins.[35,36] This result, which is far from obvious, allows composite pulse sequences obtained by ignoring spin–spin couplings to be transplanted directly to this different context.

A wide range of broadband decoupling sequences have been constructed, usually by a combination of numerical optimization and iterative expansion. The popular sequence WALTZ-16 is given in equation (34).

For the highest possible resolution, sequences have been developed which also take the homonuclear $J$ couplings into account.[37]

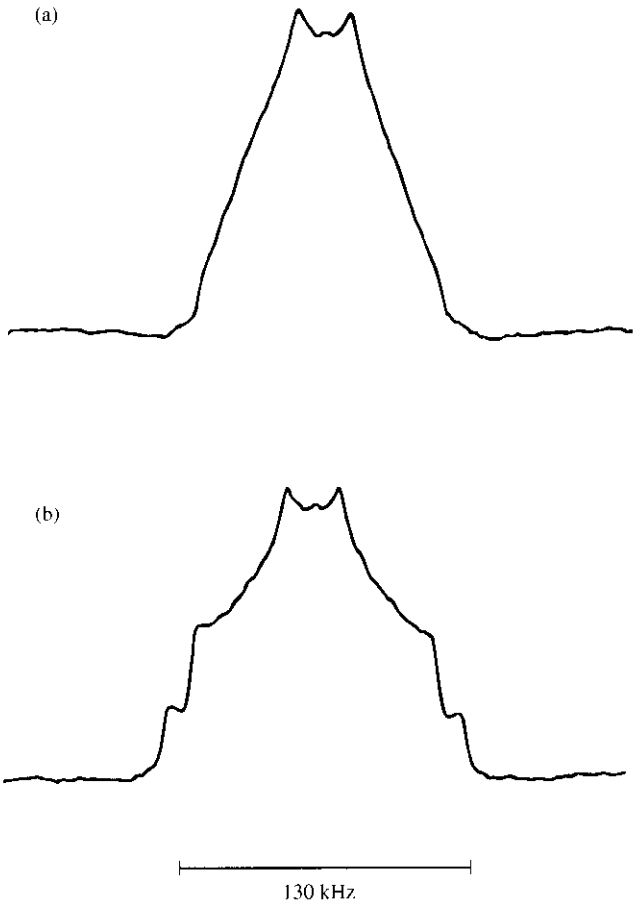


**Figure 7** $^2$H spectra of $d_5$-phenylalanine, obtained using (a) the simple quadrupole echo pulse sequence [equation (43)], and (b) a composite pulse quadrupole echo sequence [equation (44)]. The rf field was rather weak in both cases, the duration of a nominal 90° pulse being 6.2 $\mu$s. (Reproduced by permission of Elsevier from M. H. Levitt, *Prog. NMR Spectrosc.*, 1986, **18**, 61)

## 6.2 Quadrupolar Compensation

In solids, spin interactions are large, and applied rf fields face serious competition. For example, quadrupole interactions of spins $I \geqslant 1$ are generally much larger than achievable rf fields. Only for $^2$H is the quadrupolar interaction sufficiently small that the concept of an 'ideal' rf pulse is at all realistic. But even in this case, the achievable rf field is generally comparable to the quadrupolar splitting. Composite pulses can then help make up for insufficient rf field strength.

### *6.2.1 Compensated Quadrupolar Echoes*

The $^2$H NMR signals of solid powders decay very rapidly because of the strong orientation dependence of the quadrupole splitting (see ***Quadrupolar Nuclei in Solids***; ***Deuterium NMR in Solids***). To obtain undistorted signals it is usually necessary to refocus the free induction decay by a *quadrupole echo*. This involves using two 90° pulses, 90° out of phase with each other, separated by a small delay $\tau_1$:

$$90_0\text{–}\tau_1\text{–}90_{90}\text{–}\tau_2\text{–Observe} \qquad (43)$$

A spin echo is formed after an interval $\tau_2 \simeq \tau_1$ measured from the end of the second 90° pulse. Acquisition of NMR signals starting at the top of the spin echo gives high-fidelity $^2$H powder spectra.

In a disordered sample, the quadrupole splitting in high field depends on the environment and molecular orientation of the nuclear site $j$ and will be denoted here by $2\omega_Q^j$. If the rf field $\Omega_1$ is comparable to $2\omega_Q^j$, the spin transformations induced by the 90° pulses are imperfect and the spin echo is distorted. This usually appears as weakened intensity at the edges of the $^2$H powder peakshape. An example is the spectrum of $d_5$-phenylalanine shown in Figure 7(a).

To correct this effect, each 90° pulse may be replaced by a composite 90° pulse. The composite pulse must take into account the competition between the rf field and the quadrupole coupling.

Construction of such composite pulses is far from easy. In principle, the density operator for a spin $I = 1$ evolves in an eight-dimensional space. However, there is one simplifying factor. In $^2$H NMR, the chemical shifts are small. Although the frequencies of the two allowed transitions of the spin $I = 1$ nucleus are strongly orientation dependent, the *mean* frequency of the two transitions is always the same. It is possible to show that in this case, under certain constraints, quadrupole-compensated composite 90° pulses may be constructed by taking offset-compensated 180° pulses for isolated spins $\frac{1}{2}$, and dividing all pulse lengths by two.[57] The offset-compensated spin-$\frac{1}{2}$ 180° pulses must have the following properties:

1. Only 180° phase shifts must be involved.
2. Over the compensation bandwidth, the angles $\bar{\alpha}^j$ and $\gamma^j$ must depend linearly on resonance offset $\Delta\omega^j/\Omega_1^0$.

The broadband spin-$\frac{1}{2}$ composite pulses $90_0180_{180}270_0$ and $90_0270_{180}180_0360_{180}180_0$ fulfil these conditions satisfactorily over the offset range $-1.0 \leqslant \Delta\omega^j/\Omega_1^0 \leqslant 1.0$ (the latter sequence being more accurate). On halving the pulse durations, the compensated quadrupole echo sequences

$$45_090_{180}135_0-\tau_1-45_{90}90_{270}135_{90}-\tau_2-\text{Observe} \quad (44)$$

and

$$45_0135_{180}90_0180_{180}90_0-\tau_1-45_{90}135_{270}90_{90}180_{270}90_{90}-\tau_2-\text{Observe} \quad (45)$$

are constructed. The improvement in spectral appearance produced by equation (44) is illustrated in Figure 7(b). Other sequences have also been suggested.[7,57–61]

One problem of these quadrupole echo sequences is that they are rather long. Signal is lost if the coherence dephasing time $T_2$ of the deuterium spins is short due to molecular motion on a suitable timescale. This case is not uncommon. Composite pulse quadrupole echo formation is examined critically in Siminovitch et al.[61]

### 6.2.2 *Compensated Population Inversion*

Anisotropic molecular motion in solids is probed by measuring the orientation dependence of the $^2$H spin–lattice relaxation time constant $T_1$ in a powder sample. A 180° pulse is applied to disturb the spin populations, a variable waiting period $\tau_{relax}$ is left, and a quadrupole echo sequence applied to measure the NMR signal. Spectra are taken for a range of values of $\tau_{relax}$. The partially relaxed quadrupole lineshapes may be analyzed to obtain the dependence of $T_1$ on sample orientation.

This method requires proper performance of the first 180° pulse. However, a 180° pulse applied to spins $I = 1$ is very sensitive to the quadrupole splitting.[7] The transformed $z$ angular momentum $R^j_{zz}$ is below $-0.8$ only if the quadrupole splitting $2\omega^j_Q$ is less than around $1.2\Omega_1^0$, where $\Omega_1^0$ is the rf field strength. To get a reasonable inversion of a 150 kHz wide $^2$H powder pattern, the rf field must be sufficiently strong that the 90° pulse duration is less than 2 $\mu$s.

Broadband population inversion of $^2$H spins may be achieved with much weaker rf fields by using composite 180° pulses. The sequence $45_090_{180}135_045_{90}90_{270}135_{90}45_090_{180}135_0$ allows inversion of a 150 kHz quadrupole powder pattern using an rf field of only $\Omega_1^0/2\pi = 37.5$ kHz, which corresponds to a 90° pulse length of 6.5 $\mu$s.[7] Longer sequences with flatter inversion profiles have also been designed.[60] Improved performance is attainable even with the simple composite pulse $90_090_{90}90_0$.[62]

## 6.3 Dipolar Compensation

Nuclear spin dynamics are extremely complicated in the presence of extended dipolar coupling networks, as is typical for abundant spin species in solids. Compensation of these effects is even more challenging than for quadrupole couplings.

### 6.3.1 *Compensation of Homonuclear Dipolar Couplings*

Coherent averaging theory (Section 5.4.3) provides a general framework for compensation of undesirable interactions, using only the rotational symmetry of those interactions. This has allowed the development of composite pulses such as $45_0180_{90}90_{180}180_{90}45_0$, a broadband 180° pulse compensated for dipolar or quadrupolar interactions.[25] Improved population inversion has been demonstrated for networks of coupled protons in solids as well for quadrupolar spins. Composite pulses have also been constructed for NMR imaging in solids.[63]

The theory of composite pulses in dipolar-coupled systems overlaps strongly with the theory of line-narrowing multiple-pulse sequences (see ***Line Narrowing Methods in Solids***). Indeed, many of the same pulse sequences can be used. The composite pulse $90_0180_{90}90_{180}180_{90}$ is a dipolar-compensated 180° pulse as well as a segment of the line-narrowing sequence BLEW-12.[64]

### 6.3.2 *Heteronuclear Decoupling in Anisotropic Systems*

Heteronuclear decoupling in solids and liquid crystals is far more difficult than in isotropic liquids, because both homonuclear and heteronuclear interactions are generally large. Despite the theoretical difficulties, progress has been made towards the goal of low-power broadband decoupling in anisotropic systems.[65–67] One promising sequence is

$$[\mathbb{L}]_{90}[\mathbb{F}]_0[\Xi]_{90}[\mathbb{L}]_0[\mathbb{F}]_{90}[\mathbb{E}]_0[\mathbb{L}]_{270}[\mathbb{E}]_0[\Xi]_{270}[\Xi]_0[\mathbb{E}]_{270}[\Xi]_0 \quad (46)$$

where each element $\mathbb{E}$ is a constant rotation offset-compensated composite 90° pulse, $\mathbb{E} = 385_0320_{180}25_0$. Improved heteronuclear decoupling in liquid crystals and magic angle spinning solids has been demonstrated.[65–67]

## 6.4 Coherence Propagation through *J*-Coupling Networks

Another important application of composite pulse sequences is to propagate spin coherence through the $J$ coupling networks of molecules in isotropic solution. In conjunction with two-dimensional spectroscopy, such sequences are commonly used as an aid to spectral assignment. The method is generally known under the names total coherence transfer spectroscopy (TOCSY) or homonuclear Hartmann Hahn (HOHAHA) spectroscopy. A similar application is when long composite pulse sequences are used to implement coherence transfer through transverse cross relaxation—an experiment generally known under the (misleading) name rotating frame nuclear Overhauser effect spectroscopy (ROESY) (see ***ROESY***).

The theory of composite pulse sequences in this context is challenging. In particular, analysis of the relaxation during long composite pulse trains has required theoretical innovations.[68] Some of the popular pulse sequences are discussed in ***TOCSY in ROESY & ROESY in TOCSY***.

# 7 COMPENSATION FOR COUPLING VARIATIONS

In the intervals between rf pulses, evolution of the spin system takes place under the influence of chemical shifts, quadrupole couplings and spin–spin coupling terms. Many pulse sequences include fixed delays which should be matched to certain coupling constants for proper operation. For example, in the NMR of isotropic liquids, pulse sequences commonly include a fixed delay $\tau_J = 1/(2J)$ to allow exchange of anti-

For References see p. 1410

phase and in-phase coherences under the influence of the $J$ coupling. Often 180° pulses are inserted in the middle of the delay to suppress chemical shift evolution. A typical example is the INEPT sequence (see ***INEPT***) for polarization transfer from $I$ spins to $S$ spins.

$I$: $90_0$–$\tau_J/2$–$180_0$–$\tau_J/2$–$90_{90}$
$S$: $180_0$ $90_0$ (Acquire signal)

Polarization transfer is only optimal if the heteronuclear $J$ coupling really does correspond to the set delay $\tau_J$. In real samples there is a spread of $J$ values leading to a loss of polarization transfer for some sites.

This situation resembles that of a single rf pulse an inhomogeneous rf field, where the chosen pulse duration corresponds to a nominal rf field actually experienced only by a minority of spins. In that case the spread of nutation angles is compensated by making composite pulses. Similarly, the spread of $J$ couplings in polarization transfer experiments is compensated by building composite INEPT analogs.

Several research groups have investigated this.[70,71] One general procedure is explained,[70] where the following compensated sequence is demonstrated:

I: $90_0$–$\tau_J/2$–$180_0$–$\tau_J/2$–$120_{90}$–$\tau_J/2$–$180_0$–$\tau_J/2$–$30_{90}$
S: $180_0$ $180_0$ $90_{90}$ (acquire)

Although far from obvious, this composite INEPT sequence is an analog of the rf-compensated composite 90° pulse $90_0180_{120}$. The polarization transfer is less sensitive than ordinary INEPT to variations in the values of the $J$ couplings. It has also been shown that in some many-spin systems, certain $J$-compensated INEPT sequences can induce more coherence transfer than ordinary INEPT, even when the latter is at its optimum. For example, for $^1H \rightarrow {}^{13}C$ polarization transfer in $CH_3$ groups, around 33% more polarization transfer is achieved by certain composite INEPT sequences compared to ordinary INEPT.[70]

This is only one example of a large range of composite pulse sequences compensated for variations in coupling constants. Some others are as follows:

1. Hartmann–Hahn cross polarization experiments in liquids have been compensated for variations in $J$ values by making an analogy with the composite pulse $90_{90}180_0{}90_{90}$.[72]
2. Double quantum excitation sequences in liquid crystal NMR have been compensated for a range of dipolar coupling constants.[73]
3. Bilinear rotation sandwiches have been compensated for $J$ coupling variations in a whole palette of intriguing pulse schemes.[70,71,74–81]
4. Sequences for exciting quadrupolar order in solids and liquid crystals (Jeener–Broekaert sequences) have been compensated for a spread in quadrupolar coupling constants caused by orientational inhomogeneity.[82]
5. Excitation of spin magnetization in nuclear quadrupole resonance (NQR) (see ***Quadrupolar Interactions***) has been compensated for the spread of effective nutation fields caused by the orientational distribution in a powder sample.[2,3]

## 8 REFERENCES


1. A. M. Thayer and A. Pines, *J. Magn. Reson.*, 1986, **70**, 518.
2. N. Sunitha Bai, M. Ramakrishna, and R. Ramachandran, *J. Magn. Reson.* **A**, 1993, **104**, 203.
3. G. Y. Li, Y. Jiang, and X. W. Wu, *Chem. Phys. Lett.*, 1993, **202**, 82.
4. W. S. Warren and A. H. Zewail, *J. Chem. Phys.*, 1983, **78**, 2279.
5. W. S. Warren and A. H. Zewail, *J. Chem. Phys.*, 1983, **78**, 2298.
6. W. S. Warren and A. H. Zewail, *J. Chem. Phys.*, 1983, **78**, 3583.
7. M. H. Levitt, *Prog. NMR Spectrosc.*, 1986, **18**, 61.
8. T. Fujiwara and K. Nagayama, *J. Magn. Reson.*, 1988, **77**, 53.
9. M. H. Levitt and R. Freeman, *J. Magn. Reson.*, 1979, **33**, 473.
10. C. Counsell, M. H. Levitt, and R. R. Ernst, *J. Magn. Reson.*, 1985, **63**, 133.
11. A. J. Shaka and R. Freeman, *J. Magn. Reson.*, 1983, **55**, 487.
12. M. H. Levitt and R. Freeman, *J. Magn. Reson.*, 1981, **43**, 65.
13. H. W. Spiess, in 'NMR Basic Principles and Progress,' ed. P. Diehl, E. Fluck, and E. Kosfeld, Springer, Berlin, 1978.
14. There are also some composite pulses which give a fixed overall rotation over the compensation band, but for which that rotation is different from that generated by an ideal pulse. See Levitt,[7] Tycko et al.,[26] and Shaka, and Pines.[27]
15. S. Wimperis, *J. Magn. Reson.* **A**, 1994, **109**, 221.
16. M. H. Levitt and R. R. Ernst, *Mol. Phys.*, 1983, **50**, 1109.
17. M. H. Levitt and R. R. Ernst, *J. Chem. Phys.*, 1985, **83**, 3297.
18. R. Freeman, S. P. Kempsell, and M. H. Levitt, *J. Magn. Reson.*, 1980, **38**, 453.
19. M. H. Levitt, *J. Magn. Reson.*, 1982, **48**, 234.
20. M. H. Levitt, *J. Magn. Reson.*, 1982, **50**, 95.
21. B. Blümich and H. W. Spiess, *J. Magn. Reson.*, 1985, **61**, 356.
22. M. H. Levitt and R. Freeman, *J. Magn. Reson.*, 1981, **43**, 502.
23. M. H. Levitt, R. Freeman, and T. A. Frenkiel, *Adv. Magn. Reson.*, 1983, **11**, 47.
24. R. Tycko, *Phys. Rev. Lett.*, 1983, **51**, 775.
25. R. Tycko, E. Schneider, and A. Pines, *J. Chem. Phys.*, 1984, **81**, 680.
26. R. Tycko, H. M. Cho, E. Schneider, and A. Pines, *J. Magn. Reson.*, 1985, **61**, 90.
27. A. J. Shaka and A. Pines, *J. Magn. Reson.*, 1987, **71**, 495.
28. A. J. Shaka, *Chem. Phys. Lett.*, 1985, **120**, 201.
29. Z. Starčuk and V. Sklenář, *J. Magn. Reson.*, 1985, **62**, 113.
30. C. S. Poon and R. M. Henkelman, *J. Magn. Reson.*, 1992, **99**, 45.
31. N. Sunitha Bai, M. Ramakrishna, and R. Ramachandran, *J. Magn. Reson.* **A**, 1993, **102**, 235.
32. J. Baum, R. Tycko, and A. Pines, *J. Chem. Phys.*, 1983, **79**, 4643.
33. R. Tycko and A. Pines, *Chem. Phys. Lett.*, 1984, **111**, 462.
34. R. Tycko, A. Pines, and J. Guckenheimer, *J. Chem. Phys.*, 1985, **83**, 2775.
35. J. S. Waugh, *J. Magn. Reson.*, 1982, **50**, 30.
36. J. S. Waugh, *J. Magn. Reson.*, 1982, **49**, 517.
37. A. J. Shaka, C. J. Lee, and A. Pines, *J. Magn. Reson.*, 1988, **77**, 274.
38. M. H. Levitt, R. Freeman, and T. Frenkiel, *J. Magn. Reson.*, 1982, **47**, 328.
39. M. H. Levitt, R. Freeman, and T. Frenkiel, *J. Magn. Reson.*, 1982, **50**, 157.
40. More strictly, for a cycle, both $\bar{\beta}^j$ and $\bar{\xi}_\Delta{}^j$ are very small.
41. A. J. Shaka, J. Keeler, T. Frenkiel, and R. Freeman, *J. Magn. Reson.*, 1983, **52**, 335.
42. M. H. Levitt and R. R. Ernst, *J. Magn. Reson.*, 1983, **55**, 247.
43. R. Tycko and A. Pines, *Chem. Phys. Lett.*, 1984, **111**, 462.
44. R. Tycko and A. Pines, *J. Magn. Reson.*, 1984, **60**, 156.
45. A. J. Shaka and R. Freeman, *J. Magn. Reson.*, 1985, **64**, 145.
46. A. J. Shaka, J. Keeler, M. B. Smith, and R. Freeman, *J. Magn. Reson.*, 1985, **61**, 175.
47. A. J. Shaka and R. Freeman, *J. Magn. Reson.*, 1985, **63**, 596.
48. J. Baum, R. Tycko, and A. Pines, *Chem. Phys.*, 1986, **105**, 7.
49. M. H. Levitt and M. F. Roberts, *J. Magn. Reson.*, 1987, **71**, 576.


For list of General Abbreviations see end-papers

50. M. H. Levitt, J. L. Sudmeier, and W. W. Bachovchin, *J. Am. Chem. Soc.*, 1987, **109**, 6540.
51. M. H. Levitt, *J. Chem. Phys.*, 1988, **88**, 3481.
52. A. Bielecki and M. H. Levitt, *J. Magn. Reson.*, 1989, **82**, 562.
53. A. L. Davis and S. Wimperis, *J. Magn. Reson.*, 1989, **84**, 620.
54. R. Freeman, T. A. Frenkiel, and M. H. Levitt, *J. Magn. Reson.*, 1981, **44**, 409.
55. A. Bax, R. Freeman, T. A. Frenkiel, and M. H. Levitt, *J. Magn. Reson.*, 1981, **43**, 478.
56. C. J. R. Counsell, M. H. Levitt, and R. R. Ernst, *J. Magn. Reson.*, 1985, **64**, 470.
57. M. H. Levitt, D. Suter, and R. R. Ernst, *J. Chem. Phys.*, 1984, **80**, 3064.
58. T. Fujiwara and K. Nagayama, *J. Magn. Reson.*, 1991, **93**, 563.
59. D. Wang, G. Li, and X. Wu, *J. Magn. Reson.*, 1987, **74**, 464.
60. D. P. Raleigh, E. T. Olejniczak, and R. G. Griffin, *J. Magn. Reson.*, 1989, **81**, 455.
61. D. J. Siminovitch, D. P. Raleigh, E. T. Olejniczak, and R. G. Griffin, *J. Chem. Phys.*, 1986, **84**, 2556.
62. N. J. Heaton, R. R. Vold, and R. L. Vold, *J. Magn. Reson.*, 1988, **77**, 572.
63. J. B. Miller and A. N. Garroway, *J. Magn. Reson.*, 1989, **85**, 432.
64. D. P. Burum, M. Linder, and R. R. Ernst, *J. Magn. Reson.*, 1981, **44**, 173.
65. K. V. Schenker, D. Suter, and A. Pines, *J. Magn. Reson.*, 1987, **73**, 99.
66. D. Suter, K. V. Schenker, and A. Pines, *J. Magn. Reson.*, 1987, **73**, 90.
67. D. Suter, A. Pines, J. H. Lee, and G. Drobny, *Chem. Phys. Lett.*, 1988, **144**, 324.
68. C. Griesinger and R. R. Ernst, *Chem. Phys. Lett.*, 1988, **152**, 239.
69. G. A. Morris and R. Freeman, *J. Am. Chem. Soc.*, 1979, **101**, 760.
70. S. Wimperis and G. Bodenhausen, *J. Magn. Reson.*, 1986, **69**, 264.
71. O. W. Sørensen, J. C. Madsen, N. C. Nielsen, H. Bildsøe, and H. J. Jakobsen, *J. Magn. Reson.*, 1988, **77**, 170.
72. G. C. Chingas, A. N. Garroway, R. D. Bertrand, and W. B. Moniz, *J. Magn. Reson.*, 1979, **35**, 283.
73. T. M. Barbara, R. Tycko, and D. P. Weitekamp, *J. Magn. Reson.*, 1985, **62**, 54.
74. J. R. Garbow, D. P. Weitekamp, and A. Pines, *Chem. Phys. Lett.*, 1982, **93**, 504.
75. S. Wimperis and R. Freeman, *J. Magn. Reson.*, 1984, **58**, 348.
76. S. Wimperis and R. Freeman, *J. Magn. Reson.*, 1985, **62**, 147.
77. A. M. Torres, R. E. D. McClung, and T. T. Nakashima, *J. Magn. Reson.*, 1990, **87**, 189.
78. A. M. Torres and R. E. D. McClung, *J. Magn. Reson.*, 1991, **92**, 45.
79. A. M. Torres, T. T. Nakashima, R. E. D. McClung, and D. R. Muhandiram, *J. Magn. Reson.*, 1992, **99**, 99.
80. A. M. Torres, T. T. Nakashima, and R. E. D. McClung, *J. Magn. Reson.* **A**, 1993, **102**, 219.
81. A. M. Torres, T. T. Nakashima, and R. E. D. McClung, *J. Magn. Reson.* **A**, 1993, **101**, 285.
82. S. Wimperis and G. Bodenhausen, *Chem. Phys. Lett.*, 1986, **132**, 194.

## Biographical Sketch

Malcolm H. Levitt, *b* 1957. B.A., 1978, D.Phil., 1981 (supervisor: Ray Freeman), Oxford University, UK. Postdoctoral work at Weizmann Institute, Israel (with Shimon Vega), 1981–82, and ETH-Zürich, (with Richard Ernst), 1982–86. Research Associate at Francis Bitter Magnet Laboratory, Massachusetts Institute of Technology, 1986–90; Royal Society Research Fellow, Interdisciplinary Research Centre for Superconductivity, Cambridge University, UK, 1990–91. Presently Lecturer in the Physical Chemistry Division, Stockholm University. Approx. 80 publications. Current research speciality: principles and methodology of NMR in both solid and liquid phases.